Environ. Sci. Technol. **2004**, *38,* 1183−1187

Treatment of Saline Wastewater Contaminated with Hydrocarbons by the Photo-Fenton Process

JOSÉ ERMÍRIO F. MORAES,[†] FRANK H. QUINA,[‡] CLÁUDIO AUGUSTO O. NASCIMENTO,[†] DOUGLAS N. SILVA,[†] AND OSVALDO CHIAVONE-FILHO*[,§]

Departamento de Engenharia Química - Escola Politécnica, Universidade de São Paulo (USP), Cidade Universitária, São Paulo, 05508-900, SP, Brazil, Instituto de Química, Universidade de São Paulo (USP), Cidade Universitária, São Paulo, 05508-900, SP, Brazil, and Departamento de Engenharia Química - PPGEQ, Universidade Federal do Rio Grande do Norte - UFRN, Campus Universitário, Lagoa Nova, Natal, 59072-970, RN, Brazil

The application of the photo-Fenton process to the treatment of saline wastewater contaminated with hydrocarbons is investigated. Aqueous saline solutions containing raw gasoline were used as a model oil-field-produced water. The dependence on concentrations of the following reagents has been appropriately evaluated: hydrogen peroxide (100−200 mM), iron ions (0.5−1 mM), and sodium chloride (200−2000 ppm). The reactions were monitored by measurement of the absorption spectra and total organic carbon (TOC). Experimental results demonstrate that the photo-Fenton process is feasible for the treatment of wastewaters containing hydrocarbons, even in the presence of high concentrations of salt. The effect of the salt in this process is described through a series of reactions. A simple feedforward neural network model was found to correlate well the observed data for the degradation process.

Introduction

Hydrocarbons derived from petroleum are an important class of pollutants. Soil contamination from leakage due to corrosion of reservoirs and pipelines is a common occurrence in regions where fuel distributors are located. The usual method of remediation is excavation followed by transfer to an appropriate contention site or incineration. The former transfers and concentrates the pollutants without destroying them, while incineration destroys the original pollutants, but may produce secondary pollution during combustion. One possible solution of this problem would be the remediation in situ via a Fenton reaction (*1*, *2*). Another form of pollution caused by hydrocarbons occurs during extraction of petroleum from underground or undersea reservoirs. A considerable amount of water is frequently present in these reservoirs. Wastewaters produced in the extraction and oil production stages can be reinjected into the reservoir for secondary recovery of oil or, alternatively, treated before discharge into the environment. A typical treatment procedure for oceanic discharge may include the use of an electrostatic separator to retain the hydrocarbons, followed by addition of polyelectrolytes for further reduction of the organic content. In addition to being relatively inefficient for the reduction of pollutants to low levels of contamination, a high energetic cost is associated with pumping the wastewater to the oceanic discharge site. Although aliphatic hydrocarbons are usually only very slightly soluble in water, accommodation is known to be an important phenomenon in the formation of petroleum fields (*3*−*5*). Accommodation corresponds to the formation of kinetically stable systems that are not true solutions but that contain an amount of hydrocarbons in excess of their normal solubility in water. This phenomenon is influenced by several variables, including time, the presence of other hydrocarbons, and pH and is potentially a complicating factor in the systematic study of petroleum wastewater degradation.

Conventional physical-chemical and biological methods of treatment are often inadequate for treating oil-field-produced water. Furthermore, any process that requires filtration, flocculation, or adsorption can be expected to produce more concentrated petroleum residues, which in turn will require disposal by some other means. In this context, photocatalytic oxidation processes, usually known as Advanced Oxidation Processes (AOP), represent a particularly attractive alternative for treatment or pretreatment of petroleum wastewaters. AOPs are processes designed to generate hydroxyl radicals ($HO^{\bullet}$) as the primary oxidizing agent. The high oxidation potential of the hydroxyl radical (2.8 V) makes it much more efficient than other oxidizing agents such as hydrogen peroxide (1.78 V) or ozone (2.07 V). Among the various known AOPs, the photo-Fenton reaction is particularly attractive for the degradation of highly toxic and/or nonbiodegradable compounds and frequently leads to complete mineralization of the pollutant (*6*−*8*).

The photo-Fenton process utilizes a combination of hydrogen peroxide (H_2O_2) and ferrous ions (Fe^{2+}) in the presence of UV radiation. The first step of the process is the Fenton reaction (*9*, *10*), represented by eq 1.

$$Fe^{2+} + H_2O_2 \rightarrow Fe^{3+} + OH^- + HO^{\bullet} \qquad (1)$$

In the presence of UV radiation, the ferric ions (Fe^{3+}) produced in the thermal Fenton reaction are photocatalytically converted back to ferrous ions (Fe^{2+}), as shown in eq 2, with formation of an additional equivalent of hydroxyl radical.

$$Fe^{3+} + H_2O \xrightarrow{h\nu} Fe^{2+} + H^+ + HO^{\bullet} \qquad (2)$$

The hydroxyl radicals formed in these two reactions react with organic species (RH) present in the system, promoting their oxidation, as indicated in eq 3.

$$HO^{\bullet} + RH \rightarrow H_2O + R^{\bullet} \qquad (3)$$

The pH of the solution has a considerable influence on the rate of degradation. At pH values higher than four, iron ions precipitate out of solution in the form of hydroxides. The optimum pH for photo-Fenton reactions is typically in the range of pH 3−3.5 (*11*), where $Fe(OH)^{2+}$ is the predominant ferric iron species present in solution.

In the present work, aqueous saline (sodium chloride) solutions containing raw gasoline were used as a model to

* Corresponding author phone: +55-84-215-3773 ext. 216; fax: +55-84-215-3770; e-mail: osvaldo@eq.ufrn.br.

[†] Departamento de Engenharia Química - Escola Politécnica, Universidade de São Paulo (USP).

[‡] Instituto de Química, Universidade de São Paulo (USP).

[§] Universidade Federal do Rio Grande do Norte - UFRN.

10.1021/es034217f CCC: $27.50
Published on Web 01/03/2004

simulate oil-field-produced water. The efficiency of the photo-Fenton process for the degradation of hydrocarbons in wastewaters was investigated as a function of reagent concentrations and salinity.

Modeling via Artificial Neural Networks. The phenomenological treatment of a photochemical system is, in general, quite complex. This is caused by the complexity of solving the equations that involve the radiant energy balance, the spatial distribution of the absorbed radiation, mass transport, and the mechanisms of a photochemical degradation involving radical species. For these reasons, the modeling of the degradation process via artificial neural network (ANN) techniques is quite appropriate (*12*−*15*).

Neural networks possess the ability to "learn" what happens in the process without actually modeling the physical and chemical laws that govern the system. The success in obtaining a reliable and robust network depends strongly on the choice of process variables involved as well as the available set of data and the domain used for training purposes (*16*).

The neural network employed is the feedforward network which information propagates in only one direction. It is useful for stationary state and steady-state kinetic modeling. In general, the network consists of processing neurons and channels for information flow between the neurons, usually denominated interconnects. Each processing neuron receives the weighted sum of all interconnected signals from the previous layer plus a bias term and then generates an output through its sigmoidal activation function. The most widely used networks are made up of three layers, the input, hidden, and output layers. According to the literature (*17*) this network is a universal approximator.

The algorithm adopted for the learning phase was the back-propagation algorithm, which is a generalization of the steepest descent method. In the traditional gradient approach for minimizing the mean square error E with respect to the weights $W_{i,j}$, one calculates the derivatives $dE/dW_{i,j}$ and then moves in the direction of steepest descendent. This technique requires the use of all the input−output pairs to determine the gradient. The back-propagation algorithm also uses gradient information to change the weights but with only one input−output pair at a time (*18*).

Neural networks are characterized by the large number of parameters involved (weights) due to the high connectivity among the neurons. Normally the data are split into two sets. One set is used to train the network and the other to test the prediction capability. In training a network, the objective is to find an optimum set of weights. When the number of weights is greater than the number of available data, the error in fitting the nontrained data initially decreases but then increases as the network becomes overtrained. In contrast, when the number of weights is smaller than the number of data points, as in the present case, the overfitting problem is not crucial.

Experimental Methodology

Materials. Ferrous sulfate heptahydrate ($FeSO_4 \cdot 7H_2O$) and hydrogen peroxide (H_2O_2; 30%) were used as the source of hydroxyl radicals. A quenching solution containing potassium iodide (KI; 0.1 M), sodium sulfite (Na_2SO_3; 0.1 M), and sodium hydroxide (NaOH; 0.1 M) was used to interrupt the reaction in the samples. The salinity was varied by addition of sodium chloride (NaCl), and the pH was adjusted by addition of concentrated sulfuric acid (H_2SO_4). All chemical compounds were analytical grade. Raw gasoline, without additives, was employed as the model pollutant for optimizing the experimental design and analysis. Preliminary photo-Fenton degradation experiments were also performed using commercial gasoline to check the efficiency of the process.

Preparation of the Aqueous Gasoline Stock Solutions. To simulate the conditions of real hydrocarbon-containing wastewaters, raw gasoline was used to prepare saturated aqueous stock solutions having satisfactory reproducibility of the initial total organic carbon concentration (TOC, typically 120 ppmC). Thus, 200 mL of raw gasoline and 2 L of distilled water were mixed vigorously during 2 h by magnetic stirring. The mixture was then left standing until liquid phases separation had occurred (ca. 30 min), and the aqueous phase was separated and filtered twice through quantitative filter paper (2.0 μm). This stock solution was subsequently diluted to the desired initial organic carbon concentration (80−90 ppmC). It should be noted that, since raw gasoline is a multicomponent mixture, obtaining stock solutions of reproducible concentration requires the use of a fixed water−gasoline volume ratio and comparable ambient temperatures.

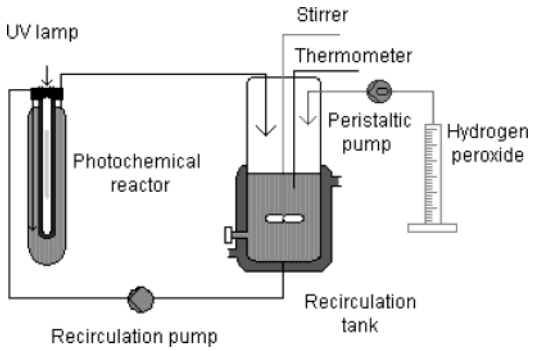

FIGURE 1. Scheme of the photochemical reactor.

Apparatus. The laboratory unit consisted of an annular photochemical reactor (net volume of 1.0 L) connected to a jacketed glass recirculation tank (volume of 1.5 L) fitted with a mechanical stirrer. The temperature of the solution was controlled by means of a thermostatic bath at 30 °C. The solution was recirculated through the reactor at a flow rate of about 1.5 L/min by means of a centrifugal pump. Aqueous hydrogen peroxide solution was added to the system at the desired flow rate by a peristaltic pump. A scheme of the photochemical reactor is shown in Figure 1. A Hannovia 450-W medium-pressure mercury vapor lamp in a water-cooled borosilicate glass immersion well was used as the light source.

Experimental Procedure. After determination of total organic carbon (TOC), the stock solution of gasoline in water was diluted to obtain 2.2 L of solution with a concentration of organics of 80−90 ppmC. The pH of this solution was adjusted to 3.0 by adding small amounts of concentrated sulfuric acid (H_2SO_4) and the salinity adjusted to the desired final value by addition of NaCl. This solution was charged into the recirculation tank and circulated with the lamp on until the temperature of the tank had stabilized at 30 °C. The photo-Fenton reaction was then initiated by addition of 100 mL of an aqueous solution of $FeSO_4 \cdot 7H_2O$, followed by the gradual addition of H_2O_2 over the first 2 h of reaction (100 mL total, at a rate of 0.83 mL/min).

Duplicate samples (5 mL each) were withdrawn for analysis at appropriate time intervals during the course of the reaction (4.5 h overall, typically 9 sampling intervals). Quenching solution (2 mL) was added to one of the two samples to interrupt the reaction, which was then filtered (0.22 μm Millipore Durapore membrane) to remove precipitated iron-containing species and analyzed for remaining total organic carbon (Shimadzu TOC-5000A TOC analyzer). The absorption spectrum of the other sample was determined on a Varian Cary 50 UV−visible spectrophotometer.

Results and Discussion

The initial exploratory experiments were carried out with commercial gasoline, which, in Brazil, contains 22−24% ethyl

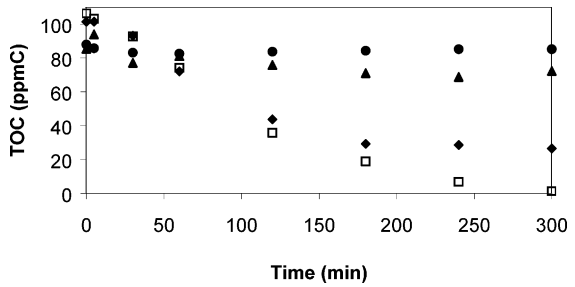

FIGURE 2. Influence of UV radiation, sodium chloride concentration, and Fenton reagents on the commercial gasoline photocatalyzed degradation in water at 30 °C; [Fe^{2+}] = 1 mM and [H_2O_2] = 100 mM: ◆ photo-Fenton process (with 1000 ppm of NaCl); □ photo-Fenton process (without NaCl); ▲ thermal Fenton reaction, and ● photolysis (without Fe^{2+} and H_2O_2).

TABLE 1. Factorial Experimental Design for Raw Gasoline Photodegradation in Water

	absolute level		
coded level	H_2O_2 (mmol/L reaction)[a]	Fe^{2+} (mM)	NaCl (mM)
−1	100	0.50	200
0	150	0.75	1100
+1	200	1.00	2000

[a] Total number of millimoles of H_2O_2 added to the recirculation tank per liter of reaction mixture.

alcohol as well as other additives. In the absence of added salt (NaCl), commercial gasoline−water mixtures could be completely mineralized. In contrast, under the same conditions (30 °C; [H_2O_2] = 100 mM; [Fe^{2+}] = 1 mM) but in the presence of salt (1000 ppm of NaCl), the mineralization of organic compounds was incomplete, reflecting an inhibition of the photo-Fenton process (*19*). These preliminary experiments also confirmed the photocatalytic nature of the process. In the absence of NaCl, the corresponding percentages of degradation were 15% for the thermal Fenton reaction without UV radiation, 3% for UV radiation in the absence of the Fenton reagents (photolysis alone), and 99% for the combined action of H_2O_2/Fe^{2+}/UV radiation (photo-Fenton system). These observations are summarized in Figure 2.

Raw gasoline (gasoline without any additives) was chosen as the starting material for the preparation of the model hydrocarbon wastewater employed in the remaining experiments. In all cases, the model effluent solutions were colorless prior to irradiation or to addition of the Fenton reagents. During the initial exposure to UV radiation, the solution turned slightly brown. Upon addition of ferrous ions and hydrogen peroxide, i.e., upon initiation of the photo-Fenton

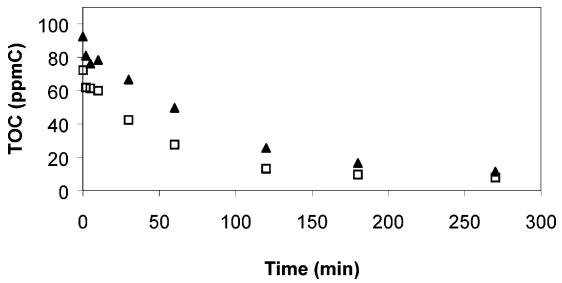

FIGURE 3. Influence of [Fe^{2+}] on raw gasoline photocatalyzed degradation in water at 30 °C; [H_2O_2] = 200 mM and [NaCl] = 2000 ppm: □ [Fe^{2+}] = 1 mM; ▲ [Fe^{2+}] = 0.5 mM.

degradation, the solution remained yellow up to ca. 10 min, before gradually fading over the subsequent 20 min. After 1 h of reaction, the solution was practically colorless and slightly cloudy, remaining so until the end of the reaction. These changes could be monitored via the absorption spectra of samples collected during the degradation, which also show the gradual loss of the bands below 265 nm, indicative of degradation of aromatic compounds, which absorb in this wavelength range.

To evaluate the dependences on the pertinent variables and generate a database for the process, a series of experiments was carried out in random sequence in accord with a two-level factorial design (2^3). Table 1 presents the coded and absolute values of the parameters used in the factorial experimental design. The experimental data for total organic carbon as a function of reaction time for all gasoline photodegradation experiments in aqueous medium are listed in Table 2. Based on three repetitions at the central point, the experimental error in the TOC measurements was estimated to be ±3.6 ppmC.

As shown in Figure 3, the initial concentration of ferric ion (Fe^{2+}) had a significant influence in the beginning on the degradation process. Thus, at the maximum amounts of hydrogen peroxide (200 mM) and sodium chloride (2000 ppm), the percent degradation at 1 h decreased from 62% to 46% upon reducing the Fe^{2+} concentration from 1.0 to 0.5 mM. In contrast, over the range studied (100−200 mM), the amount of hydrogen peroxide did not significantly influence the photodegradation performance, as shown in Figure 4. The influence of salinity was much more significant and adversely affected the photodegradation of hydrocarbons. Figure 5 presents a comparison between experiments performed with the minimum amounts of H_2O_2 and Fe^{2+} at two very different sodium chloride concentrations. At 200 ppm of NaCl, degradation reached 78% after 1 h of reaction and 90% at the end of the experiment. At 2000 ppm NaCl, the degradation was 50% after 1 h and 83% at the end of the experiment.

TABLE 2. Kinetic Data for the Photodegradation of Gasoline in Water at 30 °C

	TOC (ppmC)[a]										
time (min)	− − −	+ − +	− − +	0 0 0	+ + +	− + −	0 0 0	− + +	+ − −	0 0 0	+ + −
0	84.83	84.93	82.69	87.77	80.75	85.65	87.76	92.41	86.26	85.05	79.68
2	78.65	83.79	76.52	88.09	76.85	82.12	80.81	80.92	81.20	76.79	74.10
5	73.77	79.32	74.72	79.32	69.93	75.12	79.59	76.19	78.78	73.85	73.05
10	71.90	79.18	69.59	78.75	64.46	72.84	75.89	78.26	66.85	74.41	62.69
30	35.95	54.11	59.93	44.17	28.43	52.11	50.54	66.57	21.74	46.77	31.78
60	18.24	36.81	41.31	28.62	16.39	34.30	33.38	49.57	16.38	25.98	17.40
120	10.86	23.73	18.34	20.31	10.64	14.04	14.22	25.51	6.83	15.72	5.50
180	12.03	26.80	22.51	12.63	9.06	7.22	15.83	16.55	6.12	14.34	4.27
270	8.67	13.52	14.11	9.09	4.92	6.83	13.83	11.42	3.79	16.37	6.26

[a] The symbols −, +, and 0 correspond to the code levels in Table 1, in the order of concentration of Fe^{2+}, H_2O_2, and NaCl; for example, − − − refers to 0.50 mM Fe^{2+}, 100 mM H_2O_2, and 200 mM NaCl, and 0 refers to the central point experimental condition.

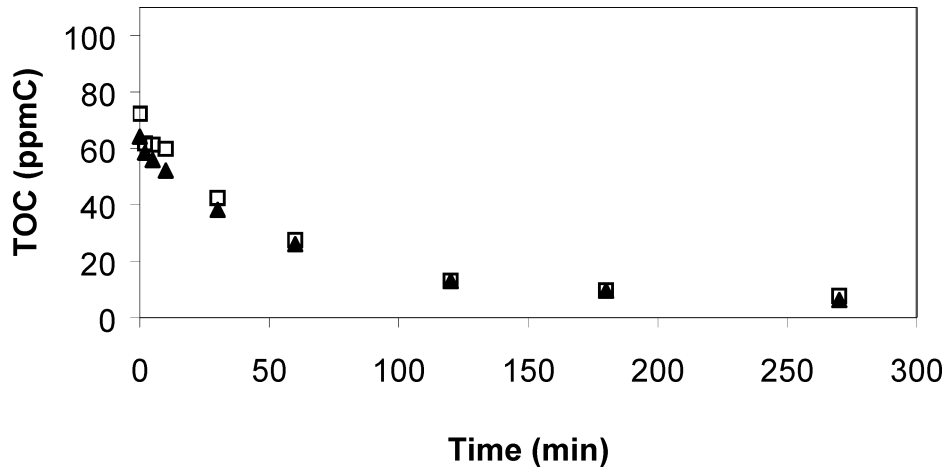

FIGURE 4. Influence of $[H_2O_2]$ on raw gasoline photocatalyzed degradation in water at 30 °C; $[Fe^{2+}] = 1$ mM and [NaCl] = 2000 ppm: □ $[H_2O_2] = 200$ mM; ▲ $[H_2O_2] = 100$ mM.

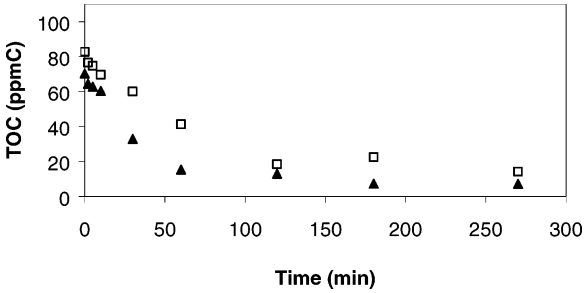

FIGURE 5. Influence of [NaCl] on raw gasoline photocatalyzed degradation in water at 30 °C; $[Fe^{2+}] = 0.5$ mM and $[H_2O_2] = 200$ ppm: □ [NaCl] = 2000 ppm; ▲ [NaCl] = 200 ppm.

The inhibitory effect of added NaCl can be understood in terms of the complexation of Fe^{3+} by Cl^- to form $FeCl^{2+}$

$$Fe^{3+} + Cl^- \rightleftarrows FeCl^{2+} \quad (4)$$

for which the equilibrium constant is 5.3 M^{-1} (*20*, *21*). Using this equilibrium constant and a pK_a of 2.7 for $Fe(H_2O)_6^{3+}$ (*20*, *21*)

$$Fe^{3+} + H_2O \rightleftarrows Fe(OH)^{2+} + H^+ \quad (5)$$

the ratio of $Fe(OH)^{2+}$ to Fe^{3+} should be approximately 2:1 under our experimental conditions (pH 3 and 2000 ppm or 0.034 M NaCl), with ca. 6−7% of the total added iron in the form of $FeCl^{2+}$. The molar absorbance of $FeCl^{2+}$ is higher than that of $Fe(OH)^{2+}$ at 366 nm, it undergoes photolysis to Fe^{2+} with a higher quantum yield (0.5 vs 0.2), and the other product is a chlorine atom rather than the hydroxyl radical (*20*, *21*):

$$FeCl^{2+} + h\nu \rightarrow Fe^{2+} + Cl^{\bullet} \quad (6)$$

Since chlorine atoms react at the diffusion controlled rate with Cl^- to form $Cl_2^{\bullet-}$ (*22*)

$$Cl^{\bullet} + Cl^- \rightarrow Cl_2^{\bullet-} \quad (7)$$

this latter is the predominant chlorine species formed under our conditions (2000 ppm added Cl^-). Although $Cl_2^{\bullet-}$ might potentially abstract hydrogen and/or react with some of the components of gasoline (e.g., toluene or xylenes) at a finite rate, its reduction potential (2.09 V vs NHE), and hence its reactivity in general, is substantially lower than that of the hydroxyl radical (*20*) for most of the components of gasoline. Thus, the observed decrease in the overall rate of degradation at the higher Cl^- concentration reflects the fact that part of the absorbed light is channeled into a pathway leading to $Cl_2^{\bullet-}$ rather than the more reactive hydroxyl radical.

Neural Network Modeling. In previous work, we have demonstrated the applicability and utility of neural network modeling methodology for the correlation of pollutant degradation data in the photo-Fenton process. In the present work, the input variables to the feedforward neural network were as follows: the reaction time (t); the initial total organic carbon (TOC_0) and the total concentrations of ferrous ions; hydrogen peroxide and sodium chloride. The total organic carbon, as a function of reaction time, was chosen as the experimental response or output variable. About 20% of the experimental data were selected randomly as the test set

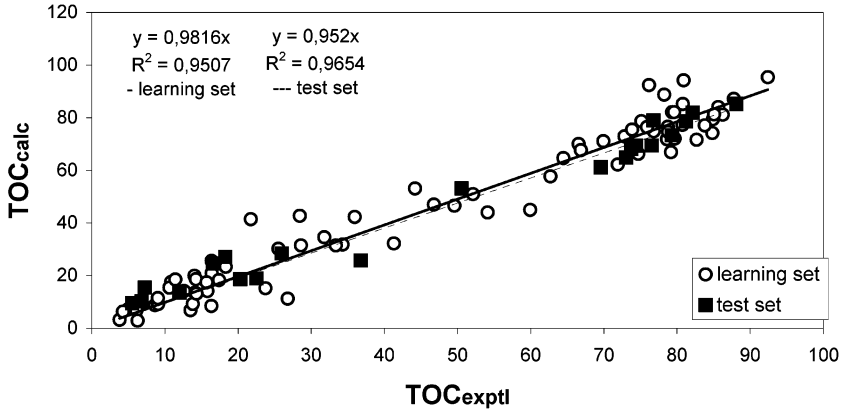

FIGURE 6. Comparison of the experimental results with those calculated via neural network modeling for the learning and test sets.

TABLE 3. Estimated Weights (Parameters) of the Neural Network for the Photodegradation Process of the Water Contaminated with Gasoline

	hidden layer		
variable	first neuron	second neuron	exit layer
time	11.948	−0.50062	first neuron
TOC_0	−1.0919	0.13793	−8.3368
$[Fe^{2+}]$	−0.46242	−0.26719	second neuron
$[H_2O_2]$	−0.25479	0.05757	9.8391
[NaCl]	0.17809	0.19678	bias
bias	0.51706	0.87187	0.4729

(TS), and the remaining data, or learning set (LS), were used to train the network and estimate the neural network parameters or weights. A neural network with 2 neurons in the hidden layer was used with 1000 iterations, providing the weights listed in Table 3.

Figure 6 shows that the performance of the final neural network is quite satisfactory for the photooxidation process of hydrocarbons. Tests were performed with more neurons in the hidden layer, but the improvement of the representation did not justify the use of more parameters. The absolute deviations for all the experimental data are symmetrically distributed around zero, as expected for a normal distribution of the error, indicating that the neural network adequately reproduces the photo-Fenton degradation process in our system. In particular, since sodium chloride concentration is one of the input variables, the neural network model is capable of reproducing the salinity effect without explicit consideration of details of the reaction mechanism.

Final Comments

The photo-Fenton reaction has been demonstrated to be an efficient process for the degradation of hydrocarbons in aqueous solution. After 4.5 h of reaction, the minimum percentage of degradation for the series of experiments was 81%. Under optimized conditions, the photodegradation reached 96%, or near total mineralization. The promising results obtained with a medium-pressure mercury lamp in a borosilicate glass photochemical reactor suggest that it should also be possible to employ solar radiation as the source of photons in the treatment of hydrocarbon-containing wastewaters. Future studies include the scale-up of this wastewater treatment, with direct monitoring of the hydrogen peroxide concentration levels, comparison of different solar reactor designs, an evaluation of the economic feasibility of the process, and identification and analysis of the principal organic intermediates produced during the photodegradation process.

Acknowledgments

Financial support and fellowships from CNPq (Conselho Nacional de Desenvolvimento Científico e Tecnológico), FAPESP (Fundação de Amparo à Pesquisa do Estado de São Paulo), ANP (Agência Nacional do Petróleo), and CAPES (Coordenação de Aperfeiçoamento de Pessoal de Nível Superior) are gratefully acknowledged.

Literature Cited

(1) Kong, S.; Watts, R. J.; Choi, J. *Chemosphere* **1998**, *37*, 1473−1482.
(2) Watts, R. J.; Haller, D. R.; Jones, A. P.; Teel, A. L. *J. Hazard. Mater.* **2000**, *76*, 73−89.
(3) Peake, E.; Hodgson, G. W. *J. Am. Oil Chemists' Soc.* **1966**, *43*, 215−222.
(4) Mcauliffe, C. *J. Phys. Chem.* **1966**, *70*, 1267−1275.
(5) Peake, E.; Hodgson, G. W. *J. Am. Oil Chemists' Soc.* **1967**, *44*, 696−702.
(6) Krutzler, T.; Bauer, R. *Chemosphere* **1999**, *38*, 2517−2532.
(7) Braun, A. M.; Oliveros, E. *Water Sci. Technol.* **1997**, *35*, 17−23.
(8) Sýkora, J.; Pado, M.; Tatarko, M.; Izakovic, M. *J. Photochem. Photobiol. A.: Chem.* **1997**, *110*, 167−175.
(9) Krutzler, T.; Fallmann, H.; Maletzky, P.; Bauer, R.; Malato, S.; Blanco, J. *Catal. Today* **1999**, *54*, 321−327.
(10) Kim, S.; Vogelpohl, A. *Chem. Eng. Technol.* **1998**, *21*, 187−191.
(11) Chen, J.; Rulkens, W. H.; Bruning, H. *Water Sci. Technol.* **1997**, *35*, 231−238.
(12) Braun, A. M.; Jakob, B.; Oliveros, E.; Nascimento, C. A. O. *Adv. Photochem.* **1993**, *18*, 253−313.
(13) Göb, S.; Oliveros, E.; Bossmann, S. H.; Straub, M.; Braun, A. M.; Guardani, R.; Nascimento, C. A. O. *Chem. Eng. Proc.* **1999**, *38*, 373−382.
(14) Nascimento, C. A. O.; Oliveros, E.; Braun, A. M. *Chem. Eng. Proc.* **1994**, *33*, 319−324.
(15) Oliveros, E.; Benoit-Marquie, F.; Puech-Costes, E.; Maurette, M. T.; Nascimento, C. A. O. *Analysis* **1998**, *26*, 326−332.
(16) Nascimento, C. A. O.; Giudici, R.; Guardani, R. Neural Network Based Approach for Optimization of Industrial Chemical Processes. *Comput. Chem. Eng.* **2000**, *24*, 2303.
(17) Cybenko, G. *Math. Control, Signals, Systems* **1989**, *2*, 303.
(18) Haykin, S. *Neural Networks − A Comprehensive Foundation*; Macmillan College Publishing Company: New York, 1994.
(19) Chen, G.; Hoag, G. E.; Chedda, P.; Nadim, F.; Woody, B. A.; Dobbs, G. M. *J. Hazard. Mater.* **2001**, *B87*, 171−186.
(20) Kiwi, J.; Lopez, A.; Nadtochenko, V. *Environ. Sci. Technol.* **2000**, *34*, 2162−2168.
(21) Nadtochenko, V.; Kiwi, J. *Environ. Sci. Technol.* **1998**, *32*, 3282−3285.
(22) Neta, P.; Huie, R. E.; Ross, A. B. *J. Phys. Chem. Ref. Data* **1988**, *17*, 1027−1284.

Received for review March 12, 2003. Revised manuscript received November 3, 2003. Accepted November 28, 2003.

ES034217F